

Cite this: DOI: 10.1039/c2lc21152a

www.rsc.org/loc

PAPER

DNA molecules descending a nanofluidic staircase by entropophoresis

Samuel M. Stavis,^{†*} Jon Geist,^a Michael Gaitan,^a Laurie E. Locascio^b and Elizabeth A. Strychalski[†]

Received 23rd November 2011, Accepted 9th January 2012

DOI: 10.1039/c2lc21152a

A complex entropy gradient for confined DNA molecules was engineered for the first time. Following the second law of thermodynamics, this enabled the directed self-transport and self-concentration of DNA molecules. This new nanofluidic method is termed entropophoresis. As implemented in experiments, long DNA molecules were dyed with cyanine dimers, dispersed in a high ionic strength buffer, and confined by a nanofluidic channel with a depth profile approximated by a staircase function. The staircase step depths spanned the transition from strong to moderate confinement. The diffusion of DNA molecules across slitlike steps was ratcheted by entropic forces applied at step edges, so that DNA molecules descended and collected at the bottom of the staircase, as observed by fluorescence microscopy. Different DNA morphologies, lengths, and stoichiometric base pair to dye molecule ratios were tested and determined to influence the rate of transport by entropophoresis. A model of ratcheted diffusion was used to interpret a shifting balance of forces applied to linear DNA molecules of standard length in a complex free energy landscape. Related metrics for the overall and optimum performance of entropophoresis were developed. The device and method reported here transcend current limitations in nanofluidics and present new possibilities in polymer physics, biophysics, separation science, and lab-on-a-chip technology.

Introduction

Nanofluidic methods to manipulate and measure biomolecules, such as DNA molecules, and other nanoscale objects have significantly impacted numerous fields, including polymer physics, biophysics, separation science, and lab-on-a-chip technology.^{1–6} Confinement and transport are fundamental to these methods, and thus the scope of nanofluidics has been limited by two common attributes.

The first is the typical fabrication of only one or two confining nanoscale structural dimensions. This restricts device functionality and results in the need for separate devices to vary the confining structural dimensions, which impedes the study and application of confinement and transport effects. A few exceptions include instances of gradual variation in confinement to funnel long DNA molecules into small channels^{7,8} and to study DNA size and confinement forces.^{9,10} These curved and tapered nanofluidic channels have not been used to control the transport of DNA molecules.

The second attribute is the usual necessity of external electrokinetic or hydrodynamic forces to transport DNA molecules through a nanofluidic device. This biases the physical

behavior of a biomolecule and the surrounding fluidic environment and introduces associated technical limitations. Interest has grown in the use of differential confinement to induce entropic forces on DNA molecules for trapping,¹¹ recoil,¹² expansion,¹³ unfolding,¹⁴ and organization.¹⁵ These entropic effects have been implemented by simple free energy landscapes established by binary confinement schemes.

Here, a novel nanofluidic functionality is introduced that transcends these common limitations. In a new type of Brownian motor, structural control over the transport and concentration of DNA molecules was implemented by complex nanofluidic confinement (Fig. 1a–b). A nanofluidic “staircase” with numerous steps¹⁶ established a complex confinement free energy landscape approximated by regions of constant confinement free energy on each slitlike step and abrupt changes in confinement free energy at the edges between steps (Fig. 1c–d). As an initial condition for “entropophoresis,” denoting transport arising from an entropy gradient, a DNA molecule was forced to ascend the staircase electrokinetically towards shallower steps. This work confined and compressed the molecule uniaxially, excluded conformational microstates, decreased conformational entropy, and increased confinement free energy. After the applied electric field was removed, the DNA molecule descended the staircase by entropophoresis towards deeper steps. In this approach towards equilibrium, uniaxial confinement decreased, conformational entropy increased, and confinement free energy decreased.

^aSemiconductor and Dimensional Metrology Division, Physical Measurement Laboratory, National Institute of Standards and Technology, Gaithersburg, MD, USA. E-mail: sstavis@nist.gov

^bBiochemical Science Division, Material Measurement Laboratory, National Institute of Standards and Technology, Gaithersburg, MD, USA

† These authors contributed equally to this publication.

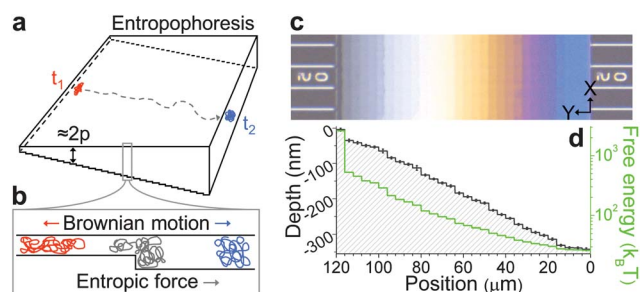


Fig. 1 Experimental concept and nanofluidic staircase. a) As an initial condition, a DNA molecule was forced electrokinetically to ascend a confining nanofluidic staircase. At t_1 , the applied external force was removed, and the DNA molecule descended the staircase by entropophoresis. At t_2 , the DNA molecule collected at the bottom of the staircase in an entropic trap. b) The DNA molecule was transported across the width of each step of the staircase by Brownian motion. Entropic forces ratcheted the DNA molecule at vertical edges between adjacent steps. c) In a brightfield optical micrograph of the empty nanofluidic device, each step of the staircase is apparent as a distinct color, due to white light interference. Connecting channels are visible at the left and right. d) The steps of the staircase (gray, average \pm standard deviation), shown to scale with the corresponding micrograph in c, established a complex confinement free energy landscape (green) for linear DNA molecules of standard length. The step depths spanned $2p$, where p is the DNA persistence length of ≈ 51 nm.

As implemented, entropophoresis resulted from a complex superposition of the physical effects of the nanofluidic confinement of DNA molecules. Some of these effects are controversial, for example the size scaling of DNA molecules in nanofluidic slits.¹⁷ Other effects have not been characterized quantitatively, such as the confinement free energy of DNA molecules in nanofluidic slits.¹⁸ Therefore, at the current state of the art, the technology introduced here leads the science. On the one hand, this prevents a complete understanding of entropophoresis. On the other hand, entropophoresis provides an experimental method to investigate these underlying physical effects. Here, a study of a shifting balance of entropic and diffusive effects that comprise entropophoresis is introduced. A related study reports quantitative measurements of the size scaling of DNA molecules in varied slitlike confinement.¹⁷ Such studies are essential to inform the rational design of nanofluidic devices incorporating slitlike structures for biopolymer analysis. The device and method reported here also form the basis of novel nanofluidic applications, such as the directed self-transport of biomolecules along complex trajectories, the directed self-patterning of biomolecular concentration gradients, and the directed self-separation of mixtures of biomolecules of different sizes and morphologies. The nanofluidic staircase is a conceptually simple but structurally complex prototype suited for the demonstration of entropophoresis. Nanofluidic devices with complex three dimensional surfaces of arbitrary design¹⁶ may be optimized for the studies and applications discussed here, as well as for other uses.¹⁹

Results and discussion

A nanofluidic channel with a depth profile approximated by a staircase function implemented complex nanofluidic

confinement. A representative brightfield optical micrograph of the staircase (Fig. 1c) and corresponding etch depths (Fig. 1d) show thirty slitlike steps with widths, w , of $4 \mu\text{m}$ and depths, d , that ranged from $(4 \pm 4) \text{ nm}$ to $(342 \pm 4) \text{ nm}$ (average \pm standard deviation). The etched and cover surfaces of the fused silica staircase had root mean square roughness values of $(2.9 \pm 0.3) \text{ nm}$ (average \pm standard deviation) and $<0.5 \text{ nm}$, respectively. The staircase was filled with 5X tris borate ethylenediaminetetraacetic acid (TBE) buffer containing 3.0% (volume fraction) 2-mercaptoethanol with a measured pH of 8.7 at $(27.0 \pm 0.1) \text{ }^\circ\text{C}$ (average \pm limit of error). The high ionic strength of this buffer resulted in electrical double layers of $<1 \text{ nm}$,^{17,20} which favored steric over electrostatic interactions between DNA molecules and the staircase and prevented a significant superposition of these different confinement effects.⁵

Entropophoresis was investigated experimentally using long dsDNA samples with linear and circular morphologies. Linear DNA molecules of a standard contour length, L , (Bacteriophage- λ , 48.5 kbp) enabled direct comparison with related studies.^{5,6} Circular DNA molecules of a comparable L (9–42 Charomid, 42.2 kbp) represented a nontrivial polymer morphology of interest in polymer physics, molecular biology, and biotechnology. DNA samples were dyed with YOYO-1 cyanine dimers. Two stoichiometric ratios of the number of DNA base pairs to dye molecules of 5 : 1 and 20 : 1 spanned the typical range found in the literature. The bis-intercalation of YOYO-1 dye molecules into a DNA molecule increased the L of the DNA molecule and may have decreased the persistence length, p , of the DNA molecule from the native value of $\approx 51 \text{ nm}$.^{5,17,21} Representative epifluorescence micrographs of individual DNA molecules from these four samples near the top and bottom of the staircase are shown in Fig. 2. The unconfined sizes of these DNA molecules, as measured by the most probable radius of gyration, R_g , ranged from $\approx (450 \text{ to } 600) \text{ nm}$ in free solution.¹⁷ As a result, DNA molecules from these four samples were always at least moderately confined by the staircase. Shorter fragments of $\approx (1 \text{ to } 10) \text{ kbp}$ and longer concatemers of linear DNA molecules of $\approx (100 \text{ to } 150) \text{ kbp}$, both dyed at a stoichiometric base pair to dye molecule ratio of 5 : 1, were also analyzed.

DNA molecules descended the nanofluidic staircase by entropophoresis, as observed by widefield epifluorescence microscopy. Fig. 3 shows the representative transport of circular DNA molecules dyed at a stoichiometric base pair to dye molecule ratio of 5 : 1. After electrokinetic initialization, DNA molecules were released at different rates, often slowly, from the shallowest step at the top of the staircase. The motion of DNA molecules along the anisotropic Y-axis of the staircase was characterized by ratcheted diffusion. In contrast, DNA molecules diffused randomly along the isotropic X-axis of the staircase. On average, the rate of transport by entropophoresis down the staircase increased rapidly until step depths $\approx (1 \text{ to } 3)p$, and then decreased gradually. For the different samples, the rate of transport was influenced by DNA morphology and size, as measured by the component of R_g projected parallel to the X–Y plane, R_{\parallel} .¹⁷ Differences in the rate of transport were most significant near the top of the staircase (Fig. 4). On average, linear DNA molecules descended the nanofluidic staircase faster

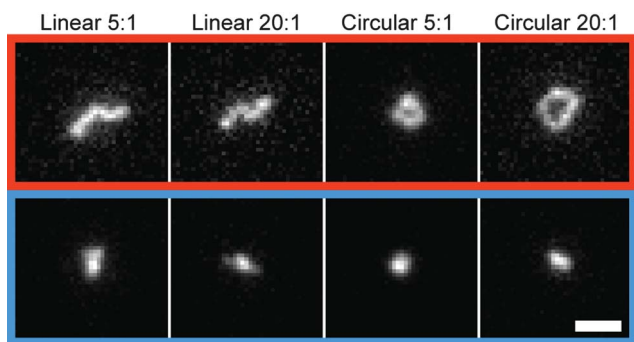


Fig. 2 DNA molecules confined to a nanofluidic staircase. Long DNA molecules were dyed with YOYO-1 at stoichiometric base pair to dye molecule ratios of 5 : 1 and 20 : 1 and dispersed in 5X TBE buffer containing 3.0% (volume fraction) 2-mercaptoethanol with a measured pH of 8.7 at $(27.0 \pm 0.1)^\circ\text{C}$ (average \pm limit of error). Widefield epifluorescence micrographs show representative linear and circular DNA molecules near the top (red) and bottom (blue) of the staircase, in strong and moderate slitlike confinement, respectively. The size of a DNA molecule, as characterized by R_{\parallel} , the component of the radius of gyration projected parallel to the image plane, decreased as the molecule descended the staircase.¹⁷ The average background intensity for each image was subtracted to aid visual comparison between molecules. The scale bar is 3 μm .

than circular DNA molecules of comparable L (Fig. 4a, 4b). For linear and circular DNA morphologies, entropophoretic transport was similar for DNA molecules dyed at the two different stoichiometric base pair to dye molecule ratios (Fig. 4a, 4b). Concatemers formed of two linear DNA molecules descended

the staircase faster on average than the individual constituent linear DNA molecules (Fig. 4a). The longest and fastest DNA molecule analyzed here was a concatemer formed of three linear DNA molecules (Fig. 5). Shorter fragments of DNA diffused throughout the staircase (not shown). Near the bottom of the staircase, transport slowed as differences between adjacent step depths became small. DNA molecules collected and concentrated near the deepest step of the staircase in an entropic trap.¹¹

To interpret the results of these experiments, several interactions between a DNA molecule and the staircase are considered (Fig. 1b). The Brownian motion of a DNA molecule spanning a step edge was ratcheted towards deeper steps by an entropic force. A DNA molecule with its entire contour length on one step diffused freely across the two unconfined dimensions of that step. As a DNA molecule descended the staircase, applied entropic forces weakened, DNA diffusivity, D , increased,^{22,23} and DNA size, R_{\parallel} , contracted.¹⁷ Drag forces occurred throughout by friction with the staircase surfaces and hydrodynamic interactions.

These effects are examined quantitatively for linear DNA molecules dyed at a stoichiometric base pair to dye molecule ratio of 5 : 1, the most standard sample investigated here. This analysis benefits from the most data obtained in previous studies, in particular for diffusivity.²³ In this way, this sample serves as a reference for the other DNA samples investigated here. This analysis is also expected to be the most relevant to future studies.

The magnitude of the entropic force applied to a DNA molecule spanning a step edge was proportional to the

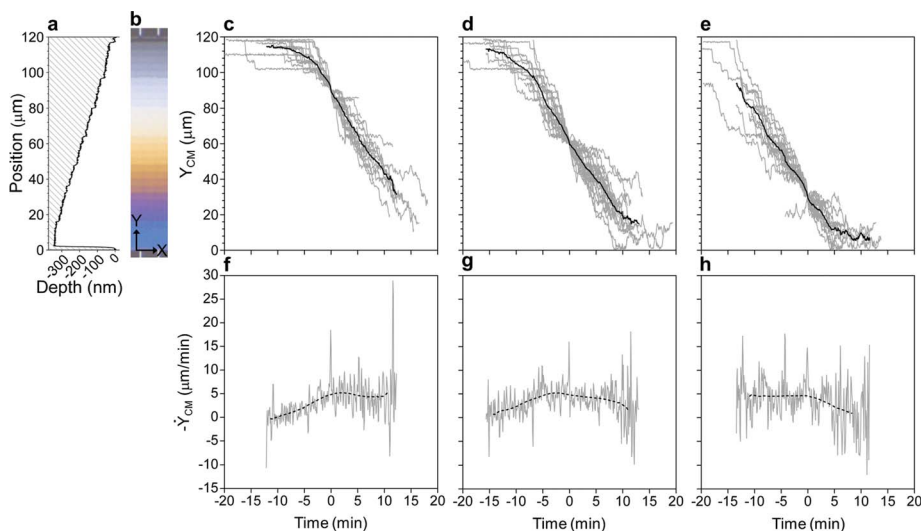


Fig. 3 DNA molecules descending a nanofluidic staircase. The various DNA samples entropophoresed down the staircase and concentrated near the deepest step in an entropic trap. a) The depth profile of the staircase and b) the corresponding optical micrograph are to scale with plots c–e, which depict transport by entropophoresis. c–e) Gray lines show the intensity-weighted center of mass positions along the y -axis, Y_{CM} , as a function of time for 59 individual circular DNA molecules dyed at a stoichiometric base pair to dye molecule ratio of 5 : 1. The uncertainty in center of mass position is smaller than the line thickness. Black lines show the averages of at least five individual trajectories. To account for different starting positions of single DNA molecules, trajectories were aligned with time equal to zero at c , $Y_{\text{CM}} = 30 \mu\text{m}$, d , $60 \mu\text{m}$, or e , $90 \mu\text{m}$, thus showing transport down the entire staircase. f–h) Gray lines show the instantaneous time derivatives of the average molecular trajectories in each plot above. To guide the eye, black dash lines depict these time derivatives smoothed by adjacent-averaging over 10 min intervals. Moving down the staircase, the average rate of transport of these DNA molecules increased until step depths $\approx (1 \text{ to } 3)p$ and then decreased gradually. Transport slowed further near the bottom of the staircase as differences in step depth decreased.

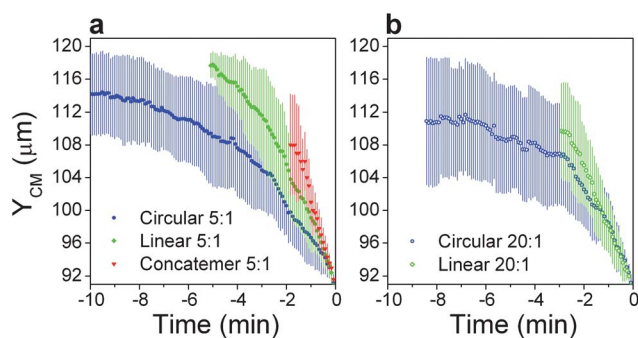


Fig. 4 Differences in the rate of transport by entropophoresis. DNA morphology and size influenced the rate of transport by entropophoresis, particularly near the top of the staircase. The intensity-weighted center of mass position (average \pm standard deviation) for at least 5 DNA molecules along the anisotropic Y-axis as a function of time is shown with time equal to zero at $Y_{CM} = 90 \mu\text{m}$. a) and b) show DNA molecules dyed with YOYO-1 at stoichiometric base pair to dye molecule ratios of 5 : 1 and 20 : 1, respectively. Linear DNA molecules entropophoresed faster on average than circular DNA molecules of comparable contour length. Concatemers formed of two linear DNA molecules descended faster than the constituent linear DNA molecules. For linear and circular morphologies, transport was similar for DNA molecules dyed at different stoichiometric base pair to dye molecule ratios.

difference in confinement free energy between adjacent steps. During entropophoresis, a DNA molecule transitioned between different limiting regimes of confinement determined by the relative values of d , p , and R_g . Near the top of the staircase, where $d \ll 2p$ imposed strong confinement, a DNA molecule was expected to behave as a series of Odijk deflection segments.^{18,24} Near the bottom of the staircase, where $2p \ll d \ll 2R_g$ resulted in moderate confinement, a DNA molecule could be described either as a flexible chain²⁵ or as a series of self-avoiding deGennes blobs.^{5,26} Near the center of the staircase around $d \approx 2p$, a wormlike chain formalism²⁷ has been used to interpolate through the transition between the strong and moderate scaling regimes of confinement and quantify the free energy of confinement F as a function of step depth d :

$$F(d) = k_B T \frac{1.6449 \left(\frac{\sqrt{2pL}}{d} \right)^2}{\left(1.2865 \left(\frac{2p}{d} \right)^2 + 0.9920 \left(\frac{2p}{d} \right) + 1 \right)^{3/2}}$$

where k_B is Boltzmann's constant, T is the absolute temperature of the solution of 300.0 K, p is the DNA persistence length assumed to be 51 nm, and L is the contour length of 23.1×10^3 nm for a linear DNA molecule of 48.5 kbp dyed at a stoichiometric base pair to dye molecule ratio of 5 : 1.⁶ This wormlike chain formalism describes confinement free energy values that decreased over two orders of magnitude down the staircase (Fig. 1d). However, this formalism does not explicitly account for excluded volume and hairpin formation.¹⁸ Both phenomena have been approximated in a scaling analysis but have unknown quantitative effects on confinement free energy¹⁸ and therefore cannot be accounted for here. Excluded volume is expected to be significant at $d < 3p$, as determined by a comparison of quantitative measurements¹⁷ and purely entropic models²⁸ of DNA size variation. As a result, this wormlike chain formalism may underestimate the free energy of confinement for $d < 3p$.

The topography of the confinement free energy landscape was determined by the relative values of R_{\parallel} and w . In the point particle limit of $R_{\parallel} \ll w$, this landscape was characterized by regions of constant free energy on each slitlike step and abrupt changes in free energy at the edges between steps. Linear DNA molecules dyed at a stoichiometric base pair to dye molecule ratio of 5 : 1 tended towards this limit, and Fig. 1d thus shows a simplified free energy landscape, which neglects the finite size of a DNA molecule¹⁷ and depicts the changes in free energy at step edges as abrupt. In practice, free energy changes and resulting entropic forces depended on spatiotemporal intramolecular and step edge interactions of a DNA molecule. In the large molecule limit of $R_{\parallel} > w$, multiple changes in free energy occurred along the length of a molecule. This influenced the transport of DNA concatemers, as described below.

A model of ratcheted diffusion was used to approximate the time required for a DNA molecule to descend the staircase. In this model, the center of mass of a DNA molecule was positioned



Fig. 5 Entropophoresis dominated by entropic forces. a) The depth profile of the staircase and b) the corresponding optical micrograph are shown to scale with c) time-lapsed widefield epifluorescence micrographs of a concatemer formed of three linear DNA molecules dyed at a stoichiometric base pair to dye molecule ratio of 5 : 1. This concatemer represents the longest and fastest DNA molecule analyzed here. Near the top of the staircase, the concatemer elongated over multiple step edges. As a result, multiple entropic forces of varied magnitude were applied to the concatemer. These forces oriented the concatemer and reduced drag in the direction of transport. Both effects tended to increase the rate of transport by entropophoresis. Moving down the staircase, the concatemer contracted but still spanned at least two steps, so that the free diffusion component of entropophoresis was eliminated. To aid comparison, these images have been background subtracted and normalized to the same intensity scale.

initially at the edge between two steps (Fig. 1b). The DNA molecule diffused across the deeper of the two steps to the next step edge down in an average time, $t = w^2/4D$. The molecule was then transferred instantly to the next deeper step, and this process was repeated. The average two dimensional diffusion time t corresponds to a probability of 0.1573 that the center of mass of a DNA molecule diffused across a step from one step edge to the next step edge. Diffusivity data from a related study²³ were used to calculate diffusion times for linear DNA molecules dyed at a stoichiometric base pair to dye molecule ratio of 5 : 1 on each step of the staircase, corrected for experimental differences in temperature and viscosity. This intuitive and quantitative model implicitly accounts for hydrodynamic drag and surface friction during diffusion, but neglects the finite size of a DNA molecule and assumes ideal ratcheting. These limitations restrict the application of this model of ratcheted diffusion as a predictive model of entropophoresis. However, the relation between theory and experiment in Fig. 6 is instructive in the interpretation of these phenomena and useful in the development of practical measures of performance.

A comparison between calculated ratcheted diffusion times and measured transport times across each step shows qualitative agreement between theory and experiment by a crossover at step depths $\approx(2 \text{ to } 3)p$ (Fig. 6). In the context of the free energy landscape for the DNA molecule (Fig. 1d), this crossover is interpreted as a force balance that demarcates two regimes of entropophoretic transport. Moving down the staircase, these regimes were characterized by a shifting balance of entropic and diffusive effects. In the more entropic regime, on steps shallower than $\approx 2p$, entropophoresis was faster than the ratcheted diffusion model. Relatively large entropic forces were applied to DNA molecules with relatively large values of R_{\parallel} .¹⁷ These effects acted in concert to abbreviate the diffusive component of entropophoresis, which was slowed by relatively small values of D . A transition occurred at step depths $\approx(2 \text{ to } 3)p$ as the differences in the free energies between the steps in this range, $\Delta F/k_B T = (18 \pm 7)$ (average \pm standard deviation), became equivalent to the thermal energy of the segments of a DNA molecule interacting with a step edge. In the more diffusive regime, on steps deeper than $\approx 3p$, entropophoresis was slower than the ratcheted diffusion model. Relatively small entropic forces were applied to DNA molecules with relatively large values of D .²³ Reduced entropic ratcheting allowed diffusive transport up onto shallower steps to occur more frequently (Fig. 3c–e). As R_{\parallel} decreased, relatively small DNA molecules diffused further across steps between entropic interactions with step edges.

This analysis provides the first and most fundamental of three performance metrics for entropophoresis reported here. Specifically, entropic control over the diffusive motion of DNA molecules of standard length was exerted optimally at slit depths $< \approx 3p$ and confinement free energy differences between adjacent steps $> \approx 20 k_B T$. This analysis was enabled by the spontaneous transport of DNA molecules down the numerous steps of the nanofluidic staircase, and the results are of general relevance to the manipulation of DNA molecules in nanofluidic slitlike confinement. The transport times in Fig. 6 provide the second and third measures of control over entropophoresis. In the second performance metric, the sum of the average transport times down the 25 steps away from the top and bottom of the

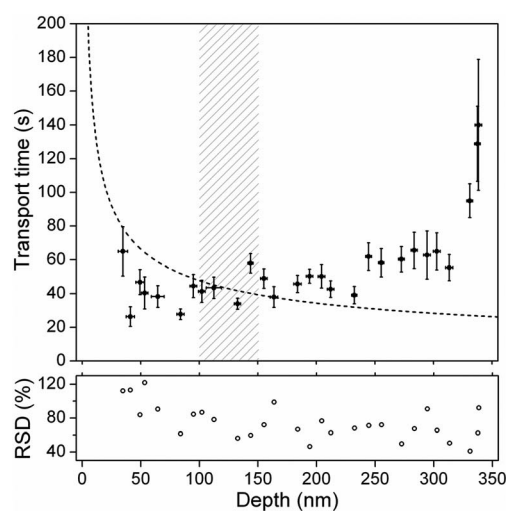


Fig. 6 A shifting balance of entropic and diffusive effects. Measured transport times (filled circles are average values, vertical bars are one standard uncertainty, horizontal bars are one standard deviation) are compared to ratcheted diffusion times (black dash line) for 115 linear DNA molecules dyed at a stoichiometric base pair to dye molecule ratio of 5 : 1. The crossover at step depths $d \approx (2 \text{ to } 3)p$ (gray hatching) indicates two regimes of transport. A transition occurred as free energy differences between adjacent steps, $\Delta F/k_B T \approx 20$, became comparable to the thermal energy of the segments of a DNA molecule interacting with a step edge. For step depths $d < 2p$, entropophoresis was faster than ratcheted diffusion. In relative terms, strong entropic forces were applied to DNA molecules with large R_{\parallel} , which abbreviated the slow diffusive component of entropophoresis. For step depths $d > 3p$, entropophoresis was slower than ratcheted diffusion. Weak entropic forces allowed diffusive transport up onto shallower steps to occur more frequently, while small DNA molecules diffused further across steps. Entropophoresis was faster than free diffusion over an equivalent submillimeter distance by a multiplicative factor of $\approx(41 \text{ to } 14)$. The relative standard deviations (RSD, empty circles) of the transport times added in quadrature show $< 20\%$ variation in entropophoresis down the entire staircase.

staircase with depths $\approx(35 \text{ to } 314)$ nm was compared to the calculated free diffusion times of DNA molecules over an equivalent distance of $100 \mu\text{m}$ in discrete slitlike channels with slit depths corresponding to the step depths. Between step depths of $\approx(35 \text{ to } 314)$ nm, the entropophoretic transport time of ≈ 20 min was faster than free diffusion over an equivalent distance by a multiplicative factor of $\approx(41 \text{ to } 14)$, respectively. This demonstrates the rapid transport of DNA molecules of a standard length over the largest ever reported submillimeter displacement induced by nanofluidic confinement. Entropophoresis may also be slower than free diffusion, for example, in the case of entropic trapping at the bottom of the staircase. In the third performance metric, the relative standard deviations of the transport times added in quadrature showed $< 20\%$ variation in entropophoresis down the entire staircase. This shows a remarkable overall measure of nanofluidic structural control over an otherwise stochastic transport process.

While a full theory of entropophoresis remains the subject of ongoing investigation, current understanding permits the following interpretations of the results reported here.

The slow release of DNA molecules from the shallowest steps at the top of the staircase is attributed to steric interactions with

surface roughness, self-entanglement, or electrostatic effects at step edges, all of which increased as slit depth decreased. These phenomena also affected the initial conformation of a DNA molecule, which influenced subsequent transport. Further study is required to discriminate between these phenomena and guide the design of nanofluidic devices optimized for the controlled release of DNA molecules from an initial condition of strong confinement.

DNA morphology, structure, and length influenced the rate of transport by entropophoresis in a complex manner, particularly near the top of the staircase. The faster descent of linear DNA molecules compared to circular DNA molecules of comparable L (Fig. 4) is attributed in part to the larger R_{\parallel} of linear DNA molecules in the same slitlike confinement¹⁷ and associated smaller effective diffusion distances and times across steps. Linear DNA molecules also encountered step edges with larger effective areas than circular DNA molecules, potentially allowing faster initiation of entropic ratcheting.^{11,29} The different stoichiometric DNA base pair to YOYO-1 dye molecule ratios of 5 : 1 and 20 : 1 resulted in significant changes to the L of the DNA molecules. However, for a given morphology, the rate of transport was similar for the different ratios (Fig. 4). This is consistent with similar measurements of R_{\parallel} for the different base pair to dye molecule ratios,¹⁷ which suggested that p decreased with increased dye concentration. Shorter DNA fragments had increased diffusivity relative to the linear DNA molecules²³ but were subjected to less conformational confinement in the regime of $R_g \ll d$. As a result, shorter fragments diffused relatively rapidly and freely throughout the staircase. Longer concatemers of DNA had decreased diffusivity relative to the linear DNA molecules²³ but assumed elongated conformations in the regime of $R_{\parallel} \gg w$ that extended across multiple step edges at the top of the staircase (Fig. 5). As a result, multiple entropic forces of varied magnitude were applied to the concatemers, which aligned these longer molecules and reduced hydrodynamic drag in the direction of entropophoresis. Moving down the staircase, longer concatemers contracted but still spanned at least two steps, which eliminated the free diffusion component of entropophoresis.

These effects emphasize a novel characteristic of the complex nanofluidic confinement scheme implemented here. For tapered or curved nanofluidic channels, a smooth gradient in confinement free energy is established. This gradient may be so shallow over the spatial extent of a DNA molecule that the diffusion of the DNA molecule is not entropically biased even in strong confinement,⁹ or so steep over the spatial extent of a DNA molecule that the diffusion of the DNA molecule into regions of even moderate confinement is entropically disfavored.¹⁰ Whatever the slope, a spatial gradient in confinement free energy induces a corresponding spatial gradient of states of DNA transportation or concentration. In contrast, the staircase structure implemented a confinement free energy landscape distinguished by abrupt changes in free energy at step edges. The number and magnitude of entropic forces applied to a DNA molecule depended strongly on the spatial relation between the size of the DNA molecule and the engineered step width and depths. In this way, complex nanofluidic confinement may be engineered to direct the self-transport and self-concentration of DNA molecules or other nanoscale objects with different sizes in

distinctly different regimes of more entropic or more diffusive behavior. This may be exploited to induce discrete spatial states of DNA transportation or concentration.

Conclusion

A complex entropy gradient was engineered to direct the self-transport and self-concentration of DNA molecules. After electrokinetic initialization, no forces were applied to DNA molecules external to those induced by complex nanofluidic confinement. Associated technological limitations, such as continuous power input, monitoring, feedback, lag, transients, heating, and engineered attachment to particles or surfaces, were eliminated. The surrounding nanofluidic environment remained static aside from hydrodynamic interactions, so that DNA molecules entropophoresed through a quiescent fluid. As implemented, transport down the staircase by entropophoresis was faster than free diffusion, but slow enough for linear and circular DNA molecules to remain near physical equilibrium on each step. This enabled a study of the size scaling of these DNA molecules in nanofluidic slitlike confinement.¹⁷ Future studies of interest include measurement of the free energy of DNA molecules in nanofluidic slitlike confinement and characterization of spatiotemporal entropic ratcheting interactions. The differences in entropophoretic transport reported here could be applied to the directed self-separation of a mixture of biomolecules of different lengths¹² or the directed self-formation of complex biomolecular concentration gradients. Entropophoresis could also be used for the directed self-transport of biomolecules past sensors for detection, functionalized surfaces for binding, or other nanoscale objects already trapped in local free energy minima^{3,15} for sequential organization. The nanofluidic staircase used to demonstrate entropophoresis is a conceptually simple but structurally complex device of arbitrary design.¹⁶ Therefore, the technology and method demonstrated here may be optimized for different analytes, studies, and applications by variation of the device design. Experimental conditions, such as buffer composition and solution temperature, may also be varied to influence transport through electrostatic effects, buffer viscosity, and analyte diffusivity. In conclusion, the device and method reported here form the basis of passive nanofluidic technology to implement the spontaneous transportation, separation, concentration, and organization of DNA molecules and other nanoscale objects in solution. This confluence of capabilities will enhance the basic scientific relevance and practical utility of nanofluidics.

Experimental

Device fabrication and characterization

A thin film of photoresist coated on a fused silica substrate was exposed to a pattern of stepped grayscale intensities, as implemented by a chromium-on-quartz photomask used in conjunction with a reduction photolithography system as a diffraction filter. An etch mask with a depth profile approximated by a staircase function was formed as the partially exposed photoresist was fully developed. A reduced staircase structure pattern was transferred into the fused silica substrate with a low selectivity reactive ion etch. Inlet and outlet holes were blasted through the substrate with micro-abrasive media. The

nanofluidic staircase was enclosed by a fused silica cover with a thickness of $\approx 170 \mu\text{m}$ bonded and annealed to the fused silica substrate. Before bonding, the etched surface of the staircase was quantitatively characterized by scanning probe surface profilometry and atomic force microscopy. After bonding, the nanofluidic staircase was qualitatively characterized by white light interferometry. Possible uncertainties in device dimensions due to the hydration or dissolution of silica were neglected. Details of the fabrication and characterization processes are reported elsewhere.^{16,19}

Device preparation

Polyethylene fluid reservoirs were attached to the substrate wafer using silicone adhesive. Voltage for electrokinetic drive was applied by platinum wires inserted into the fluid reservoirs. The nanofluidic device was initially filled by capillarity with a mixture of 90% (volume fraction) ethanol and 10% (volume fraction) 18 M Ω cm deionized water filtered to 20 nm. Prior to each experiment, each device reservoir was rinsed thrice with deionized water and filled with a fresh solution of 5X tris borate ethylenediaminetetraacetic acid (TBE) buffer¹⁷ (Fluka BioChemika) containing 3.0% (volume fraction) 2-mercaptoethanol (Fluka BioUltra) with a measured pH of 8.7 at $(27.0 \pm 0.1)^\circ\text{C}$ (average \pm limit of error). The device was then rinsed for 1 h by electrokinetic flow. Following each experiment, the device was rinsed for at least 1 h by electrokinetic flow and stored under 5X TBE buffer solution.

Sample preparation and handling

Linear DNA (Bacteriophage- λ , 48.502 kbp, New England Biolabs) and circular DNA (9–42 charomid, 42.2 kbp, Wako) molecules were dyed with YOYO-1 iodide (Invitrogen), a dimeric cyanine fluorescent dye, at DNA base pair to fluorescent dye molecule stoichiometric ratios of 5 : 1 and 20 : 1 in 5X TBE and stored at 4°C . The DNA molecules had native contour lengths of $16.5 \mu\text{m}$ (linear) and $12.9 \mu\text{m}$ (circular), assuming 0.34 nm/bp , and a native persistence length of 51 nm .²¹ The bis-intercalation of fluorescent dye molecules increased the DNA contour lengths, L , by 0.68 nm per dye molecule⁶ and altered the persistence length, p , in an uncertain manner.^{6,20,30} Frozen stock solutions of DNA and dye molecules were received from the manufacturers and thawed to room temperature. Dilutions of the stock dye solution in 5X TBE buffer were made according to the concentrations needed for the desired degrees of labeling. DNA molecules were added to the appropriate dye solutions for a final concentration of $5 \mu\text{g mL}^{-1}$ and stored at room temperature for 1 h followed by 50°C for 2 h to effect uniform labeling. Prior to loading into the nanofluidic device, dyed DNA solutions were heated to 65°C for 10 min to reduce concatemerization of linear DNA molecules. Solutions containing DNA molecules were pipetted using large-diameter pipette tips and a mechanical apparatus to stabilize all fluid handling equipment to minimize fragmentation of the DNA molecules due to viscous shear stress.

Fluorescence microscopy

All experiments were imaged with an inverted optical video-microscope operated in widefield epifluorescence mode. A metal

halide short arc lamp was used in conjunction with a 450 nm to 490 nm bandpass filter for fluorescence excitation, and a 495 nm dichroic mirror was used with a 500 nm to 550 nm bandpass emission filter to isolate fluorescence emission. A plan apochromat microscope objective lens with a magnification of $63\times$ and a numerical aperture of 1.4 was used to include the entire $120 \mu\text{m}$ y -axis of the staircase within the field of view and the maximum $\approx 350 \text{ nm}$ z -axis depth of the staircase within the depth of focus. A water-cooled electron multiplying charge coupled device camera with a pixel size of $(16 \times 16) \mu\text{m}$ held at a head temperature of -80°C was used to obtain images of DNA molecules descending the nanofluidic staircase with 40 ms exposures at (1 or 5) s time lapse intervals, with the excitation light shuttered between image acquisitions. A microscope incubator enclosed and held the nanofluidic device and critical optomechanical elements at a constant experimental temperature of $(27.0 \pm 0.1)^\circ\text{C}$ (average \pm limit of error).

Experimental procedure

After the device was rinsed, the fluid reservoirs were filled with $75 \mu\text{L}$ of 5X TBE containing 3.0% (volume fraction) 2-mercaptoethanol, and the reservoirs were covered to prevent evaporation. Care was taken to pipette equal fluid volumes into each reservoir to prevent a volumetric imbalance resulting in hydrostatic pressure-driven flow through the nanofluidic device, as verified by measurements of the free diffusion of DNA molecules along the isotropic X -axis of the staircase. Dyed DNA molecules were diluted directly in the sample inlet reservoir to a concentration of $150 \text{ ng } \mu\text{L}^{-1}$. The sample was driven slowly into the nanofluidic staircase by an electrokinetic force applied at low voltages to prevent residual electric fields from affecting the motion of DNA molecules during entropophoresis. The applied electric field was removed, and the DNA molecules were imaged over a period of $\approx (10 \text{ to } 20) \text{ min}$ as described above. All DNA molecules were imaged while descending the same region of the nanofluidic staircase structure; a representative portion of this region is shown in Fig. 1(c–d). Fresh DNA molecules were driven into the staircase prior to the start of each time-lapsed image acquisition.

Image analysis

Image analysis was performed using custom software. Linear and circular DNA molecules dyed at stoichiometric base pair to dye molecule ratios of 5 : 1 and 20 : 1 were tracked in each frame using a region of interest (ROI) around the molecule of (40×40) pixels for linear DNA molecules and (18×18) pixels for circular DNA molecules. Within the ROI, Otsu's method³¹ was used to segregate background from image, and connected regions containing ≥ 8 pixels were identified as comprising the molecule. Assuming homogeneous labeling, the mass of DNA in each pixel was proportional to the pixel intensity, which allowed calculation of an intensity-weighted center of mass.²³ Identification of the center of mass and size of the molecule was robust against photobleaching.¹⁷ Fragments and concatemers of DNA were identified by area, summed intensity, and maximum extension. Concatemers formed of linear DNA molecules dyed at a stoichiometric base pair to dye molecule ratio of 5 : 1 were analyzed

by a method similar to that described by Tang *et al.*³² For each image, a ROI was defined around the concatemer. The average background intensity was calculated from the intensity values of the pixels at the perimeter of the ROI and then subtracted from every pixel in the ROI. The standard deviation, σ , was calculated for an assumed Poisson distribution of background intensity values. A threshold intensity of $n\sigma$ was defined, where n ranged from 1.25 to 2.5 and depended on the signal to noise ratio of the image. To identify the pixels of interest that comprised the concatemer, a (3×3) and (4×4) pixel area was defined around each pixel of the ROI. The average intensity was calculated from the pixels at the perimeters of these areas. If either of these average intensity values from the perimeters was less than $n\sigma$, the pixel of interest was set to an intensity of zero and excluded from the area of the concatemer. If both average values were greater than $n\sigma$, then the pixel of interest was included in the area of the concatemer. The intensity-weighted center of mass of the concatemer was then calculated.

Transport analysis

DNA transport was analyzed using two complementary methods. In the first method, the center of mass positions of single DNA molecules along the anisotropic Y-axis of the staircase as a function of time were averaged, and this average was differentiated. To guide the eye in Fig. 3f–h, the resulting average rate of transport was smoothed by adjacent-averaging over intervals of 10 min. In the second method, the transport time of each DNA molecule across each step of the staircase was measured, and then the average, standard deviation, and standard uncertainty of the transport time distribution were calculated for each step. This latter method facilitated comparison of transport times by entropophoresis and the model of ratcheted diffusion in Fig. 6.

Diffusivity calculation

A previous study²³ of the free diffusion of DNA molecules in slitlike nanofluidic channels was used to calculate diffusivities on each step of the staircase for linear DNA molecules dyed at a stoichiometric base pair to dye molecule ratio of 5 : 1. The experimental system in the previous study was very similar to the one described here. Identical DNA samples were dispersed in TBE 5X buffer containing 4.0% (volume fraction) 2-mercaptoethanol. Slitlike nanofluidic channels with varied depths were fabricated discretely in identical fused silica wafers using a similar CHF₃/O₂ reactive ion etch process. For these discrete nanoslits, the root mean square etched surface roughness values of <1 nm were slightly smoother than the value of <3 nm used here, while the root mean square cover surface roughness values of <0.5 nm were identical. Aside from nanofluidic structure geometry, the primary differences between the previous and current experimental systems were a nominal 22 °C *versus* 27.0 °C solution temperature and a 4.0% *versus* 3.0% concentration (volume fraction) of 2-mercaptoethanol. Both of these differences influenced DNA diffusivity, $D(T) \propto T/\eta(T)$, where T is the absolute temperature and $\eta(T)$ is the kinematic viscosity. To account for these differences, the kinematic viscosity of each buffer system was measured using an Ubbelohde viscometer

submerged in a heat bath at the corresponding experimental temperature, as controlled by a refrigerated and heated water circulator with a stability of 0.1 °C and monitored independently by a thermometer with a precision of 0.1 °C. In conjunction with measurements of buffer density at the corresponding experimental temperature, it was determined that the buffer system used in the previous study had a dynamic viscosity of $(1.449 \times 10^{-3} \pm 0.004 \times 10^{-3})$ Pa·s (average \pm standard deviation), while the buffer system used here had a dynamic viscosity of $(1.254 \times 10^{-3} \pm 0.004 \times 10^{-3})$ Pa·s (average \pm standard deviation). From the previous study, diffusivities of $(0.041 \pm 0.002) \mu\text{m}^2 \text{s}^{-1}$, $(0.047 \pm 0.002) \mu\text{m}^2 \text{s}^{-1}$, $(0.068 \pm 0.003) \mu\text{m}^2 \text{s}^{-1}$, $(0.16 \pm 0.012) \mu\text{m}^2 \text{s}^{-1}$ (average \pm standard deviation), which corresponded to channel depths of 28 nm \pm 4%, 45 nm \pm 1%, 91 nm \pm 1%, 547 nm \pm 1% (average \pm standard deviation), respectively, were fit to a single power law model. This function was used to calculate the diffusivity, D , for a linear DNA molecule dyed at a stoichiometric base pair to dye molecule ratio of 5 : 1 on each step of the staircase, which was then corrected for the higher temperature and lower viscosity of the buffer system used here.

Disclaimer

Official contribution of the National Institute of Standards and Technology; not subject to copyright in the United States. Certain commercial equipment, instruments, or materials are identified to specify adequately the experimental procedure. Such identification implies neither recommendation nor endorsement by the National Institute of Standards and Technology nor that the materials or equipment identified are necessarily the best available for the purpose.

Acknowledgements

This work was performed in part while S.M.S. and E.A.S. held National Research Council Research Associateship Awards. Device fabrication was performed at the Cornell Nanoscale Science and Technology Facility (CNF), a member of the National Nanotechnology Infrastructure Network, and the Cornell Center for Materials Research, both supported by the National Science Foundation. Device characterization was performed in part at the National Institute of Standards and Technology Center for Nanoscale Science and Technology. The authors gratefully acknowledge the staff of the CNF staff for assistance with device fabrication.

References

- 1 W. D. Volkmuth and R. H. Austin, *Nature*, 1992, **358**, 600–602.
- 2 J. Han and H. G. Craighead, *Science*, 2000, **288**, 1026–1029.
- 3 M. Krishnan, N. Mojarad, P. Kukura and V. Sandoghdar, *Nature*, 2010, **467**, 692–U675.
- 4 S. L. Levy and H. G. Craighead, *Chem. Soc. Rev.*, 2010, **39**, 1133–1152.
- 5 G. B. Salieb-Beugelaar, K. D. Dorfman, A. van den Berg and J. C. T. Eijkel, *Lab Chip*, 2009, **9**, 2508–2523.
- 6 F. Persson and J. O. Tegenfeldt, *Chem. Soc. Rev.*, 2010, **39**, 985–999.
- 7 H. Cao, J. O. Tegenfeldt, R. H. Austin and S. Y. Chou, *Appl. Phys. Lett.*, 2002, **81**, 3058–3060.
- 8 E. A. Strychalski, S. M. Stavis and H. G. Craighead, *Nanotechnology*, 2008, **19**.
- 9 F. Persson, P. Utko, W. Reisner, N. B. Larsen and A. Kristensen, *Nano Lett.*, 2009, **9**, 1382–1385.

- 10 S. R. Leslie, A. P. Fields and A. E. Cohen, *Anal. Chem.*, 2010, **82**, 6224–6229.
- 11 J. Han, S. W. Turner and H. G. Craighead, *Phys. Rev. Lett.*, 1999, **83**, 1688–1691.
- 12 M. Cabodi, S. W. P. Turner and H. G. Craighead, *Anal. Chem.*, 2002, **74**, 5169–5174.
- 13 C. H. Reccius, J. T. Mannion, J. D. Cross and H. G. Craighead, *Phys. Rev. Lett.*, 2005, **95**, 4.
- 14 S. L. Levy, J. T. Mannion, J. Cheng, C. H. Reccius and H. G. Craighead, *Nano Lett.*, 2008, **8**, 3839–3844.
- 15 W. Reisner, N. B. Larsen, H. Flyvbjerg, J. O. Tegenfeldt and A. Kristensen, *Proc. Natl. Acad. Sci. U. S. A.*, 2009, **106**, 79–84.
- 16 S. M. Stavis, E. A. Strychalski and M. Gaitan, *Nanotechnology*, 2009, **20**, 165302.
- 17 E. A. Strychalski, J. Geist, M. Gaitan, L. E. Locascio and S. M. Stavis, *Macromolecules*, 2012, in press.
- 18 T. Odijk, *Phys. Rev. E: Stat., Nonlinear, Soft Matter Phys.*, 2008, **77**, 060901.
- 19 S. M. Stavis, J. Geist and M. Gaitan, *Lab Chip*, 2010, **10**, 2618–2621.
- 20 E. A. Strychalski, H. W. Lau and L. A. Archer, *J. Appl. Phys.*, 2009, **106**, 024915.
- 21 C. Bouchiat, M. D. Wang, J. F. Allemand, T. Strick, S. M. Block and V. Croquette, *Biophys. J.*, 1999, **76**, 409–413.
- 22 A. Balducci, P. Mao, J. Y. Han and P. S. Doyle, *Macromolecules*, 2006, **39**, 6273–6281.
- 23 E. A. Strychalski, S. L. Levy and H. G. Craighead, *Macromolecules*, 2008, **41**, 7716–7721.
- 24 T. Odijk, *Macromolecules*, 1983, **16**, 1340–1344.
- 25 P. G. de Gennes, *Scaling Concepts in Polymer Physics*, 1985 edn, Cornell University Press, Ithaca and London, 1979.
- 26 M. Daoud and P. G. Degennes, *J. Phys.*, 1977, **38**, 85–93.
- 27 J. Z. Y. Chen and D. E. Sullivan, *Macromolecules*, 2006, **39**, 7769–7773.
- 28 S. M. Stavis, E. A. Strychalski and J. Geist, *Submitted*, 2011.
- 29 K. D. Dorfman, *Rev. Mod. Phys.*, 2010, **82**, 2903–2947.
- 30 C. U. Murade, V. Subramaniam, C. Otto and M. L. Bennink, *Biophys. J.*, 2009, **97**, 835–843.
- 31 N. Otsu, *IEEE Trans. Syst. Man Cybern.*, 1979, **9**, 62–66.
- 32 J. Tang, S. L. Levy, D. W. Trahan, J. J. Jones, H. G. Craighead and P. S. Doyle, *Macromolecules*, 2010, **43**, 7368–7377.